# Copper Immobilization on Fe3o4@Agar: An Efficient Superparamagnetic Nanocatalyst for Green Buchwald-Hartwig Cross-coupling Reaction of Primary and Secondary Amines With Aryl Iodide Derivatives

**Kimia Hoseinzade**
Ferdowsi University of Mashhad
**Seyed Ali Mousavi-Mashhadi**
Ferdowsi University of Mashhad
**Ali Shiri** ( alishiri@um.ac.ir )
Ferdowsi University of Mashhad https://orcid.org/0000-0002-5736-6287

**Research Article**

**Keywords:** Agar, Buchwald-Hartwig reaction, C-N Cross-coupling, Green chemistry, Nano Fe3O4, Water

**Posted Date:** May 28th, 2021

**DOI:** https://doi.org/10.21203/rs.3.rs-559140/v1

# Abstract

Immobility of copper on magnetic nanoparticles was performed using surface rectification of $Fe_3O_4$ with Agar. The magnetic $Fe_3O_4$@Agar-Cu nanocatalyst was prepared and entirely characterized by different analyses such as Fourier transform infrared (FT-IR), X-ray diffraction (XRD), scanning electron microscopy (SEM), transmission electron microscopy (TEM), vibrating sample magnetometry (VSM), energy dispersive X-ray (EDX), thermogravimetric (TGA), and inductively coupled plasma (ICP). The nanocatalyst was applied in C-N bond formation through the cross-coupling reaction of aryl halides with primary or secondary amines in water as a green medium known as the Buchwald-Hartwig reaction. The results of the Buchwald-Hartwig reaction by $Fe_3O_4$@Agar-Cu magnetic nanoparticles as catalyst demonstrate excellent activity and stability in water. Moreover, this catalyst can be recycled several times without considerable loss in its activity.


# 1. Introduction

In recent decades, the lack of green processes in the chemical fields and industries is a significant concern. Green Chemistry is effective for human health and necessary to protect the environment.[1,2] Concern of pollutions, toxicity, and waste treatment methods are an essential issue for all chemists to use neat solvents, especially water, in their chemical processes because of the availability, recyclability, thermal stability and chemical conditions.[3–5]

There is lots of investigation to find a better catalyst, ligand, base, or more effective solvents for the Buchwald-Hartwig reaction known as C-N cross-coupling. Considering an influential catalyst that can be utilized for both primary and secondary amines and act as a regiospecific catalysts in satisfying yields have been investigating very much.[6–10] The Buchwald-Hartwig is an essential reaction since aryl amines are commonly used in pharmaceutical treat, materials, and drugs with interesting electronic properties.[11] *Neratinib* was approved in 2017 for the expanded attendant treatment of positive breast cancer (**Fig. 1-I**). *Abemaciclib* as a cyclin-dependent kinase inhibitor, is used for the treatment of breast cancer. $Pd_2(dba)_3$ can catalyze the Buchwald-Hartwig reaction to achieve the *Abemaciclib* drug (**Fig. 1-II**). [12]

Recently, the use of catalysts in many forms is a primary topic in Organic chemistry. Especially, using magnetite as one of the best support surfaces is guaranteed some properties such as the control of unwanted reactions, the stability of PH, the simplicity of the separation method and reusing of the catalyst several times, high surface area and low toxicity.[13–19]

The first catalyst that represented for Buchwald-Hartwig reaction was the Pd metal complex by organic or inorganic ligands that were accepted as the best catalyst in recent years.[20–22] Stephen L. Buchwald and coworkers reported efficient catalysts for the catalytic amination of a wide variety of aryl halides and triflates in 2000.[23] The palladium-catalyzed amination of aryl halides had been successfully known as an important method for the Buchwald-Hartwig C-N cross-coupling reaction. A variety of catalysts

represented for this reaction such as ($Fe_3O_4$@PDA/Pd(II) )[24], ($Zn(OAc)_2$)[25], (NiCl(bpy)(IPr))[26]. There are still limitations in some processes affiliated with transition metal, specifically using Pd[27–33], for example, using these high-cost metals and the difficult process in the workup.[34] In the study of the reaction, Cu is one of the most incredible noble element that can be replaced by Pd metal. Agar as a plentiful, non-toxic, cheap, and natural biopolymer, is considered as a linker for this kind of catalyst.[35–41] It can be found in the cell wall of some red algae and its strong gelling seaweed hydrocolloid composed[42]. Hitherto, the main structure of Agar-Agar is chemically characterized by the repeating units of d-galactose and 3,6-anhydro-l-galactose. Also, it has a chiral surface with free hydroxyl groups that could act as hydrogen bond donors or acceptors.[41,43]

Based on the above information and our previous studies[22,44–46], we represent an effective nanocatalyst to perform the Buchwald-Hartwig reaction by considering $Cu^{(0)}$ as a priceless and new catalyst with fascinating properties in comparison with palladium, agar as the linker, and magnetite as the support. (Scheme 1 & 2)

# 2. Results And Discussion

### 2.1. The preparation and characterization of the catalyst

The catalyst was prepared according to Scheme 1. The nano magnetite ($Fe_3O_4$ NPs) was synthesized according to the literature.[13] The agar polysaccharide was immobilized around the prepared $Fe_3O_4$ NPs. Then, copper was incorporated successfully among the agar linker at the same time. The catalyst structure was characterized using different analyses, including FT-IR, XRD, SEM, TEM, VSM, EDX, and TGA.

In **Fig. 2**, the FT-IR spectrum demonstrated the absorptions of Agar (1070 $cm^{-1}$) appear along with a peak at 582 $cm^{-1}$ which corresponds to the stretching vibration band of the Fe-O group in $Fe_3O_4$@Agar. This indicates that magnetic $Fe_3O_4$ NPs were coated by Agar. Possible bindings of copper with OH group in $Fe_3O_4$@Agar-Cu NPs have decreased the combined intensity of hydroxyl peaks at 3356 $cm^{-1}$. Splitting of the bending bands of hydroxyl at 1614 $cm^{-1}$ and 1352 $cm^{-1}$ also indicate the bonding of Cu with OH moiety. The variations in the region of 1350 $cm^{-1}$ and 1000 $cm^{-1}$ can be attributed to the perturbation in C-O vibrations induced by Agar-Cu complexation (**Fig. 2**).

The XRD patterns help define the crystal structures of $Fe_3O_4$@Agar NPs and $Fe_3O_4$@Agar-Cu NPs. Sharp peaks vouch for the excellent crystallinity of the prepared samples (**Fig. 3**). For $Fe_3O_4$@Agar NPs, the outcome is in agreement with the standard patterns of inverse cubic spinel magnetite ($Fe_3O_4$) crystal structure, showing six diffraction peaks at $2\theta$ about 35.5°, 43.3°, 56.9°, 62.6°, 62.8°, and 74.1° marked by their corresponding indices (3 1 1), (4 0 0), (3 3 3), (4 0 4), (4 0 4), and (5 3 3), respectively. The small and weak broad bands in the span of 21°–28° indicate the existence of Agar. Diffraction patterns of the $Fe_3O_4$@Agar-Cu NPs exhibit three additional peaks at $2\theta$ about 43.3°, 50.2°, and 74.1°; corresponding to (1

1 1), (2 0 0), and (2 0 2) planes of face-centered cubic (fcc) copper crystal structure. No impurities in the XRD patterns infer the formation of net $Fe_3O_4$ and Cu nanoparticles.

SEM imaging of the nanoparticles shows nanometer-sized particles of less than 25 nm in diameter. **Fig. 4** shows the morphology of the $Fe_3O_4$@Agar-Cu nanoparticles with a core–shell structure and spherical form.

TEM image of the catalyst has been shown in **Fig. 5**. The spherical shape of each nanoparticle corresponded to the core of the catalyst, similar to SEM image which can be observed at a scale of less than 25 nm. Also, TEM images show that magnetic nanoparticles of $Fe_3O_4$ have been encapsulated by the biopolymeric network of Agar.

Magnetic hysteresis measurements of $Fe_3O_4$@Agar (**Fig. 6a**) and $Fe_3O_4$@Agar-Cu (**Fig. 6b**) NPs were created in the limited area −15000 to 15000 Oe using VSM. As shown in **Fig. 6**, the saturation magnetization of $Fe_3O_4$@Agar-Cu NPs is anent 35 emu $g^{-1}$, lower than that of $Fe_3O_4$@Agar (33 emu $g^{-1}$). The magnetization curve displays that the $Fe_3O_4$@Agar-Cu NPs have paramagnetic attributes in which the nanoparticles can be easily separated from the reaction melange using an external magnet.

To specify the elemental composition of $Fe_3O_4$@Agar-Cu NPs, EDX analysis was fulfilled (**Fig. 7**). The EDX pattern supports excellent dispersion of $Fe_3O_4$@Agar-Cu NPs. Chemical characterization of the nanoparticles showed that they were composed of iron, carbon, oxygen, and copper elements, and this analysis detect the presence of 7.21 mol% Cu in $Fe_3O_4$@Agar-Cu NPs.

TGA of $Fe_3O_4$@Agar-Cu NPs was manipulated in the range of 20–550 ºC (**Fig .8**). The first mass loss of $Fe_3O_4$@Agar-Cu NPs at below 190 ºC is due to the removal of physically adsorbed water. The second and the major weight loss of $Fe_3O_4$@Agar-Cu NPs in the range of 200$^{o}$C to 380$^{o}$C is ascribed to Agar as the organic moiety.

### 2.2. Catalytic application of $Fe_3O_4$@Agar-Cu catalyst

After the characterization of the catalyst structure, the new prepared catalyst efficiency has been investigated in the Buchwald-Hartwig reaction. Initially, in order to optimize the model reaction conditions of iodobenzene with aniline, some parameters, including solvents, amounts of catalyst, temperature and the time of reaction were scrutinized thoroughly. (Table 1) The impact of the catalyst was inspected with different amounts of $Fe_3O_4$@Agar-Cu. The reaction did not proceed in the absence of the catalyst even after 15 h. The effect of solvents was also examined by polar and nonpolar solvents, including DMSO, DMF, Toluene and water. Fortunately, a high yield was observed in $H_2O$ as a green and sustainable solvent. The effect of time duration and temperature on the model reaction was also evaluated, and it was found the best time and temperature are considered as 12 h in 100 ºC with excellent yield.

Next, in order to expand the scope of this reaction, various derivatives of C-N bond cross-coupling reactions have been represented in Table 2. Considering both primary and secondary arylamines was the wisdom of this catalyst that is not previously usual. There are not any significant differences in reaction yields considering various amines (primary or secondary) bearing electron-donating or electron-with drawing groups, and all related products were obtained in good to excellent yields. Also, for improving the validity of the synthesis field and larger scale of the reaction, coumarins (entry 16 and 17) were considered as complicated amine structures. They were conducted in Buchwald-Hartwig amination reaction using $Fe_3O_4$@Agar-Cu NPs as the catalyst. The results showed magnificent success and remarkable yields based on confirmation by Mass spectroscopy, $^1H$, and $^{13}C$ NMR analyses.

As it is presented in Table 3, the comparison of this catalyst with some recently published catalysts has been performed. Various conditions have been applied, but the use of green and nontoxic reaction conditions has not been reported. Employing reachable and no harmful materials, achieving high yields of product, and mild reaction condition is the art of this study.

To check the catalyst's reusability on the model reaction, the nanocatalyst was removed easily from the mixture after the termination of the reaction, washed with ethanol and deionized water successively, and dried in vacuum oven. Soon afterward, the catalyst applied directly for the next run. Providentially, this catalyst was reused for five times and shown good revenue in the reaction process by the use of ICP analyses without significant leaching of Cu NPs (**Fig. 9**).

The possible mechanism of C-N cross-coupling represents in **Fig. 10**. The proceed mechanism is the same as C-C cross-coupling reactions.[13] Including oxidative addition of the aryl halide to a $Cu^0$ nanoparticle, the addition of the amine to the oxidative addition complex, deprotonation followed by reductive elimination of the species intermediate releases the desired product amines and complete the reaction cycles.

# 3. Experimental

### 3.1. Preparation of Agar-coated magnetic nanoparticles: $Fe_3O_4$@Agar NPs

$Fe_3O_4$@Agar magnetic nanoparticles were synthesized by dissolving a mixture of $FeCl_3.6H_2O$ (9.2 mol, 2.46 g) and $FeCl_2.4H_2O$ (4.6 mol, 0.91 g) in deionized water (150 ml) under vigorous stirring. Then, $NH_4OH$ solution (25% w/w, 10 ml) was added dropwise to the stirring mixture under the argon's atmosphere. Afterward, the solution of Agar (1.5 g) in water (50 ml) was added slowly to this mixture. The resulting solution is mechanically stirred for 5 h at 70 $^o$ C under the $N_2$ atmosphere. The resulting black material was separated using magnetic decantation and washed with deionized water (3 × 20 ml), and dried at 40 ºC for 48 h.

### 3.2. Synthesis of copper nanoparticles coated magnetic Agar: $Fe_3O_4$@Agar-Cu NPs

$Fe_3O_4$@Agar (0.8 g) was dispersed in deionized water (80 ml) in an ultrasonic bath for 15 min. Then, an aqueous solution of $CuCl_2$ (50 g/lit) is added dropwise over, for 15 min at room temperature. The mixture is mechanically stirred for the other 3 h. Subsequently, $NaBH_4$ (500 mg) is gently added to the mixture and stirred for 4 h. The color of the solution is changed from colorless to dark brown during the reaction. Eventually, $Fe_3O_4$@Agar-Cu NPs are separated by an external magnet, washed several times with water, and dried in a vacuum desiccator at room temperature.

### 3.3. General procedure for C-N cross-coupling reactions

To a mixture of primary amine or secondary amine derivative (1 mmol) and the appropriate aryl iodide (1.1 mmol) in water (0.5 ml for primary amines and 4 ml for secondary amines) and $K_2CO_3$ (1 mmol for primary amines and 2 mmol for secondary amines), $Fe_3O_4$@Agar-Cu NPs (10 mol%) was added, and the mixture is refluxed at 100 ºC for 12 h. The progress of the reaction was monitored by TLC. After completing the reaction, the catalyst was separated using an external magnet, and the crude product is extracted from the aqueous phase by EtOAc. Finally, the pure products were isolated using column chromatography on silica gel using n-hexane/EtOAc as eluent.

## Conclusion

In conclusion, we have demonstrated a noble, stable, versatile, and unique catalyst named $Fe_3O_4$@Agar-Cu NPs replaced for specific Buchwald-Hartwig catalyst reaction that usually used expensive and inaccessible Pd metal. Considering Agar as a pure and natural linker and also water as an eco-friendly solvent made this reaction undoubtedly a Green process. There is no harsh condition and surpass than the old method. More importantly, this catalyst effort both primary and secondary amines with significant yields that represent various derivatives.

## Declarations


### Acknowledgment:

The authors gratefully acknowledge the Research Council of Ferdowsi University of Mashhad (3/52357).


### Selected data:

7,7-dimethyl-5-oxo-4-phenyl-2-(phenylamino)-5,6,7,8-tetrahydro-4H-chromene-3-carbonitrile(Table 2,entry 16): white solid: mp 208-212 ºC.

$^1$H NMR(300 Hz, $CDCl_3$) δ (ppm):1.21 (s, 6H, $CH_3$),1.80 (s,1H,CH),2.58 (s,2H,$CH_2$),3.30 (s, 2H, $CH_2$), 7.23–7.62 (m, 10H, Ar–H).

$^{13}$C NMR (76 MHz, CDCl3) δ (ppm):195.1, 150.9, 131.2, 130.6, 129.0, 128.8, 128.5, 127.5, 119.4, 115.0, 58.3, 53.1, 43.6, 33.2, 30.9, 28.2.

# References


1. E. Eidi, M.Z. Kassaee, P.T. Cummings, Res. Chem. Intermed. **44**, 5787 (2018)
2. R.A. Sheldon, Green Chem. **7**, 267 (2005)
3. F. Schroeter, J. Soellner, T. Strassner, Organometallics **37**, 4267 (2018)
4. M. Sarmah, M. Mondal, U. Bora, ChemistrySelect **2**, 5180 (2017)
5. Y.H. Liu, H.C. Hu, Z.C. Ma, Y.F. Dong, C. Wang, Y.M. Pang, Monatshefte Fur Chemie **149**, 551 (2018)
6. M.M. Heravi, Z. Kheilkordi, V. Zadsirjan, M. Heydari, M. Malmir, J. Organomet. Chem. **861**, 17 (2018)
7. H. Hammoud, M. Schmitt, E. Blaise, F. Bihel, J.J. Bourguignon, J. Org. Chem. **78**, 7930 (2013)
8. P.A. Forero-Cortés, A.M. Haydl, Org. Process Res. Dev. **23**, 1478 (2019)
9. H. Christensen, S. Kiil, K. Dam-Johansen, O. Nielsen, M.B. Sommer, Org. Process Res. Dev. **10**, 762 (2006)
10. A.R. Hajipour, M. Check, Z. Khorsandi, Appl. Organomet. Chem. **31**, 1 (2017)
11. M.S.S. Adam, F. Ullah, M.M. Makhlouf, J. Am. Ceram. Soc. **103**, 4632 (2020)
12. A.C. Flick, C.A. Leverett, H.X. Ding, E. McInturff, S.J. Fink, C.J. Helal, C.J. O'Donnell, J. Med. Chem. **62**, 7340 (2019)
13. S.A. Mousavi Mashhadi, M.Z. Kassaee, E. Eidi, Appl. Organomet. Chem. **33**, 1 (2019)
14. Z. Li, S. Ji, Y. Liu, X. Cao, S. Tian, Y. Chen, Z. Niu, Y. Li, Chem. Rev. **120**, 623 (2020)
15. A. De Cattelle, A. Billen, W. Brullot, T. Verbiest, G. Koeckelberghs, J. Organomet. Chem. **899**, 120905 (2019)
16. V.T. Trang, L.T. Tam, N. Van Quy, T.Q. Huy, N.T. Thuy, D.Q. Tri, N.D. Cuong, P.A. Tuan, H. Van Tuan, A.T. Le, V.N. Phan, J. Electron. Mater. **46**, 3381 (2017)
17. Q. Zhao, C. Qian, X.Z. Chen, Monatshefte Fur Chemie **144**, 1547 (2013)
18. S. Bagheri, F. Pazoki, I. Radfar, A. Heydari, Appl. Organomet. Chem. **34**, 1 (2020)
19. S.A. Mousavi-mashhadi and A. Shiri, 3941 (2021)
20. A. Aranyos, D.W. Old, A. Kiyomori, J.P. Wolfe, J.P. Sadighi, S.L. Buchwald, J. Am. Chem. Soc. (1999)
21. H. Christensen, S. Kiil, K. Dam-Johansen, O. Nielsen, Org. Process Res. Dev. **11**, 956 (2007)
22. M. Keyhaniyan, A. Shiri, H. Eshghi, A. Khojastehnezhad, New J. Chem. **42**, 19433 (2018)
23. J.P. Wolfe, H. Tomori, J.P. Sadighi, J. Yin, S.L. Buchwald, J. Org. Chem. **65**, 1158 (2000)
24. H. Veisi, P. Sarachegol, S. Hemmati, Polyhedron **156**, 64 (2018)
25. R. Ayothiraman, S. Rangaswamy, P. Maity, E.M. Simmons, G.L. Beutner, J. Janey, D.S. Treitler, M.D. Eastgate, R. Vaidyanathan, J. Org. Chem. **82**, 7420 (2017)

26. T. Inatomi, Y. Fukahori, Y. Yamada, R. Ishikawa, S. Kanegawa, Y. Koga, K. Matsubara, Catal. Sci. Technol. **9**, 1784 (2019)
27. M. Esmaeilpour, J. Javidi, J. Chinese Chem. Soc. **62**, 614 (2015)
28. V. Mishra, A. Arya, T.S. Chundawat, Curr. Organocatalysis **7**, 23 (2019)
29. F. Dai, Q. Gui, J. Liu, Z. Yang, X. Chen, R. Guo, Z. Tan, Chem. Commun. **49**, 4634 (2013)
30. A.H. Dardir, P.R. Melvin, R.M. Davis, N. Hazari, M. Mohadjer Beromi, J. Org. Chem. **83**, 469 (2018)
31. V. Kandathil, B.D. Fahlman, B.S. Sasidhar, S.A. Patil, S.A. Patil, New J. Chem. **41**, 9531 (2017)
32. L.J. Gooßen, B. Zimmermann, T. Knauber, Angew. Chemie - Int. Ed. **47**, 7103 (2008)
33. F. Bedos-Belval, A. Rouch, C. Vanucci-Bacqué, M. Baltas, Medchemcomm **3**, 1356 (2012)
34. R. Fareghi-Alamdari, M.S. Saeedi, F. Panahi, Appl. Organomet. Chem. **31**, 1 (2017)
35. C. Zhang, Y. Dai, Y. Wu, G. Lu, Z. Cao, J. Cheng, K. Wang, H. Yang, Y. Xia, X. Wen, W. Ma, C. Liu, Z. Wang, Carbohydr. Polym. **234**, 115882 (2020)
36. E. Rafiee, A. Ataei, S. Nadri, M. Joshaghani, S. Eavani, Inorganica Chim. Acta **409**, 302 (2014)
37. M.M. Mian, G. Liu, B. Yousaf, B. Fu, R. Ahmed, Q. Abbas, M.A.M. Munir, L. Ruijia, J. Environ. Sci. (China) **78**, 29 (2019)
38. T. Baran, N. Yılmaz, Baran, A. Menteş, Int. J. Biol. Macromol. **115**, 249 (2018)
39. O.L. Kang, M. Ghani, O. Hassan, S. Rahmati, N. Ramli, Food Hydrocoll. **42**, 304 (2014)
40. Y. Hou, X. Chen, Z. Chan, R. Zeng, Process Biochem. **50**, 1068 (2015)
41. X.L. Chen, Y.P. Hou, M. Jin, R.Y. Zeng, H.T. Lin, J. Agric. Food Chem. **64**, 7251 (2016)
42. Y.P. Yew, K. Shameli, M. Miyake, N.B.B. Ahmad Khairudin, S.E.B. Mohamad, T. Naiki, K.X. Lee, Arab. J. Chem. **13**, 2287 (2020)
43. R. Armisén, F. Galatas, Handb. Hydrocoll. Second Ed. 82 (2009)
44. M. Keyhaniyan, A. Shiri, H. Eshghi, A. Khojastehnezhad, Appl. Organomet. Chem. **32**, 1 (2018)
45. Z. Ghadamyari, A. Shiri, A. Khojastehnezhad, S.M. Seyedi, Appl. Organomet. Chem. **33**, 1 (2019)
46. Z. Ghadamyari, A. Khojastehnezhad, S.M. Seyedi, A. Shiri, ChemistrySelect **4**, 10920 (2019)
47. X. Tian, J. Lin, S. Zou, J. Lv, Q. Huang, J. Zhu, S. Huang, Q. Wang, J. Organomet. Chem. **861**, 125 (2018)
48. C.A. Fleckenstein, H. Plenio, Chem. - A Eur. J. **13**, 2701 (2007)
49. S.K. Kashani, J.E. Jessiman, S.G. Newman, Org. Process Res. Dev. (2020)

# Tables

Due to technical limitations, table 1 to 3 is only available as a download in the Supplemental Files section.

# Figures

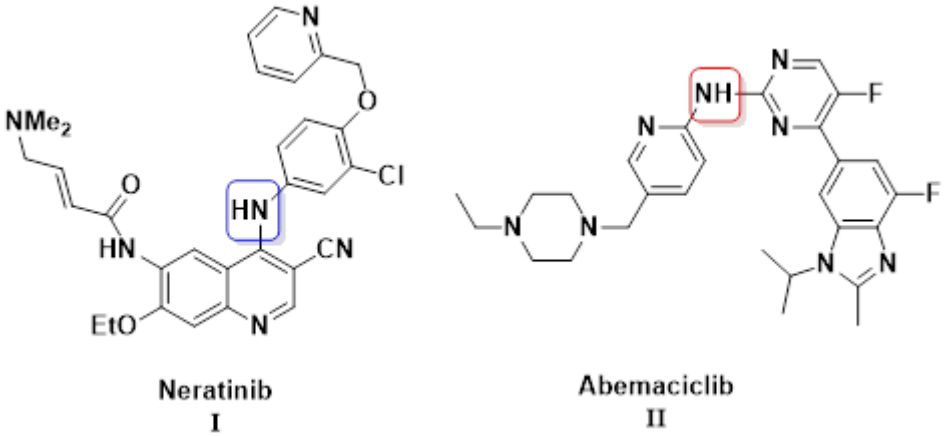


## Figure 1

Examples of Buchwald-Hartwig reaction in dugs treatment


## Figure 2

FT-IR spectrum of a) Fe3O4@Agar NPs and b) Fe3O4@Agar-Cu NPs.

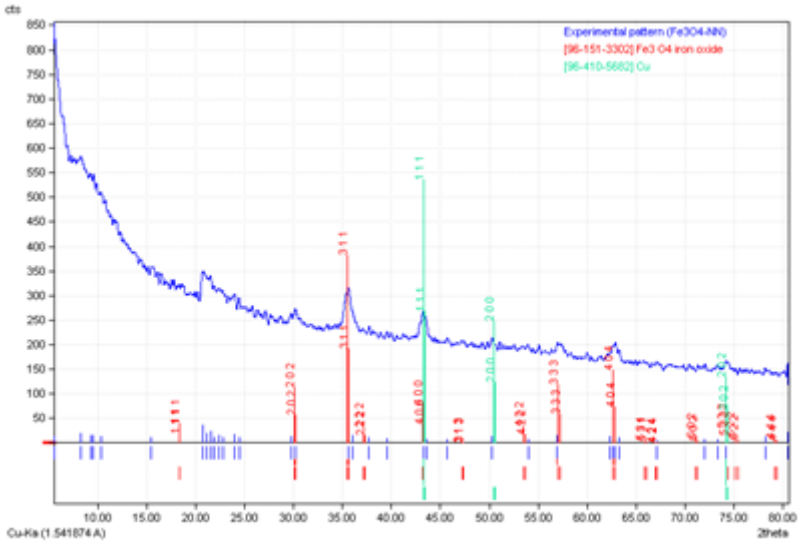


## Figure 3

X-ray diffraction spectroscopy for Fe3O4@Agar-Cu NPs

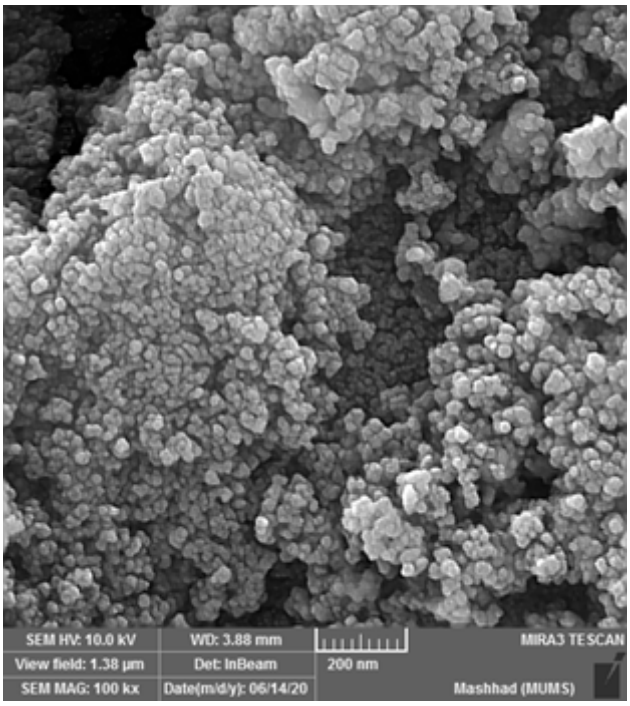


## Figure 4

Scanning electron microscopy (SEM) for Fe3O4@Agar-Cu NPs at 200 nm.

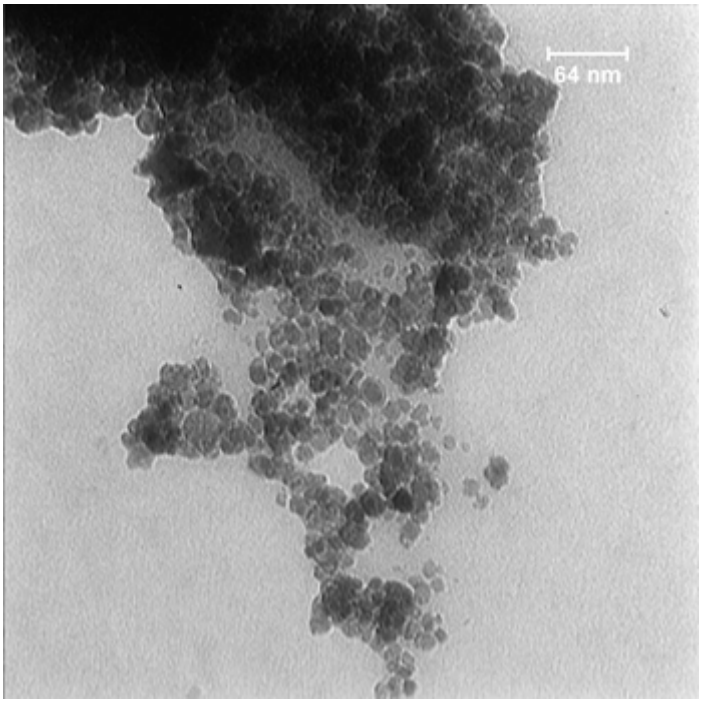


## Figure 5

Transmission electron microscopy (TEM) for Fe3O4@Agar-Cu NPs at 64 nm.

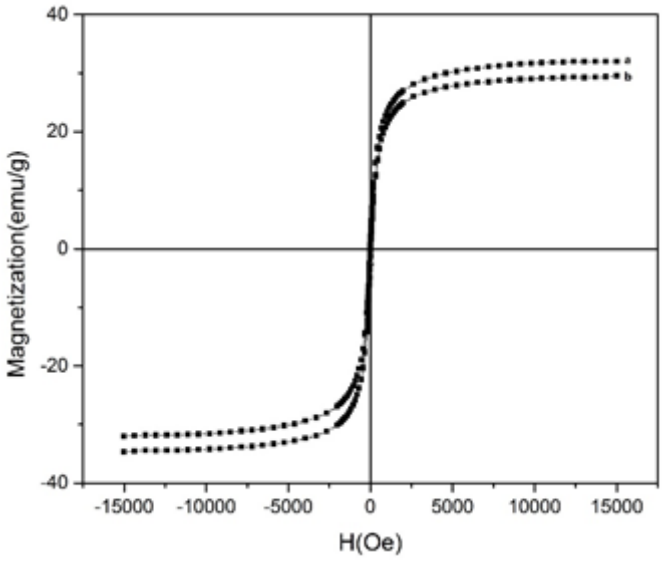


## Figure 6

Vibrating-sample magnetometer (VSM) spectroscopy a) Fe3O4@Agar and b) Fe3O4@Agar-Cu NPs.

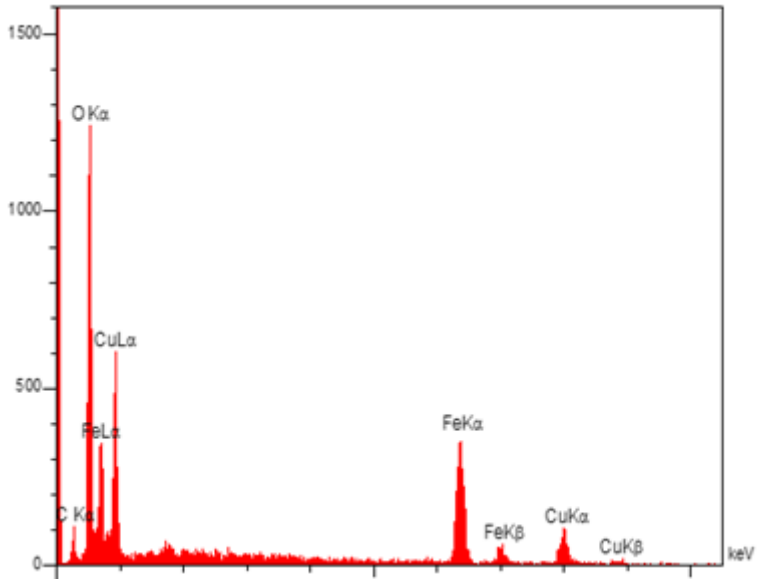


## Figure 7

Energy-dispersive X-ray spectroscopy for Fe3O4@Agar-Cu NPs.

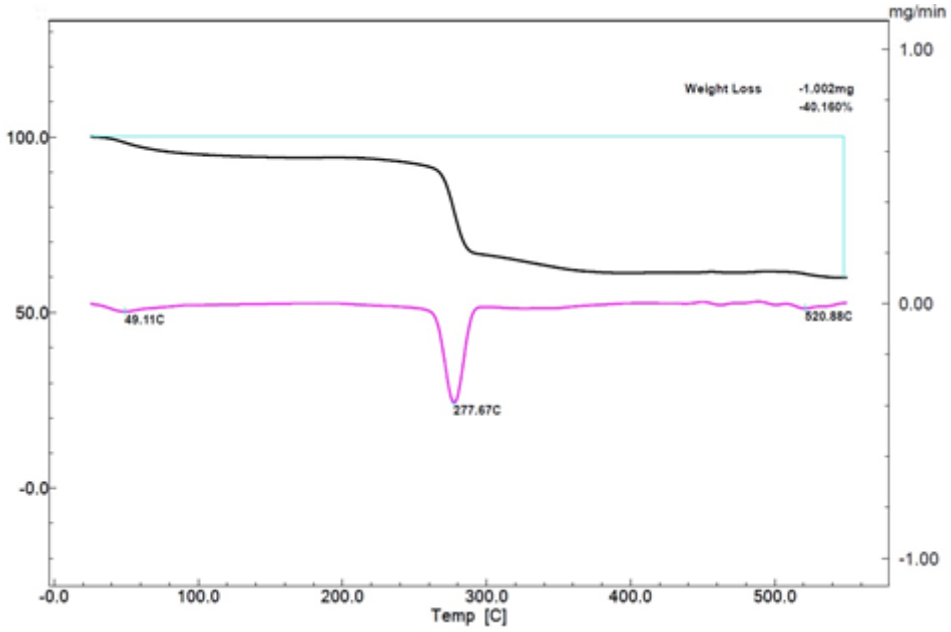


## Figure 8

Thermogravimetric analysis of Fe3O4@Agar-Cu NPs.

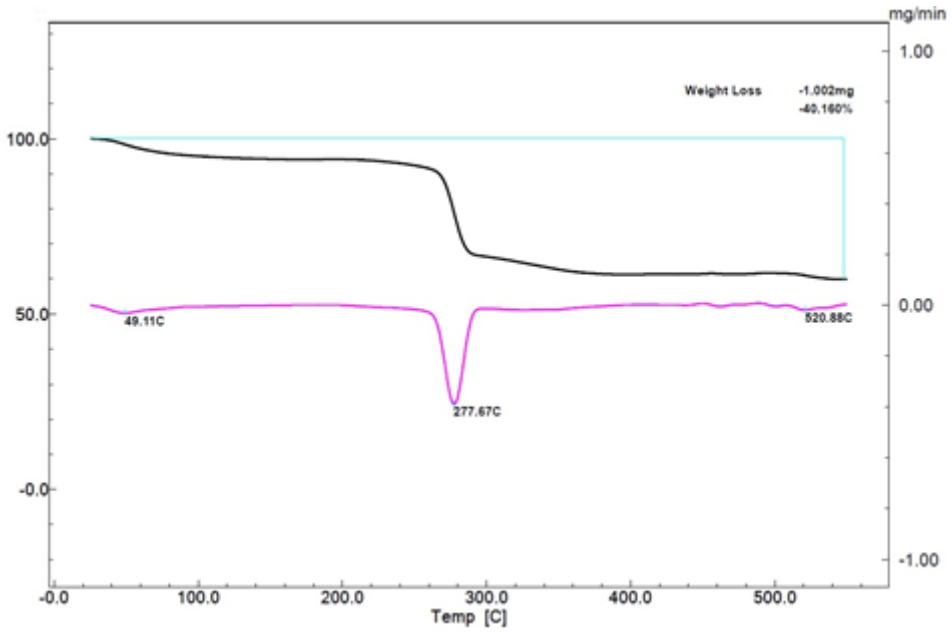


## Figure 9

Reusability of the catalyst for the model reaction.

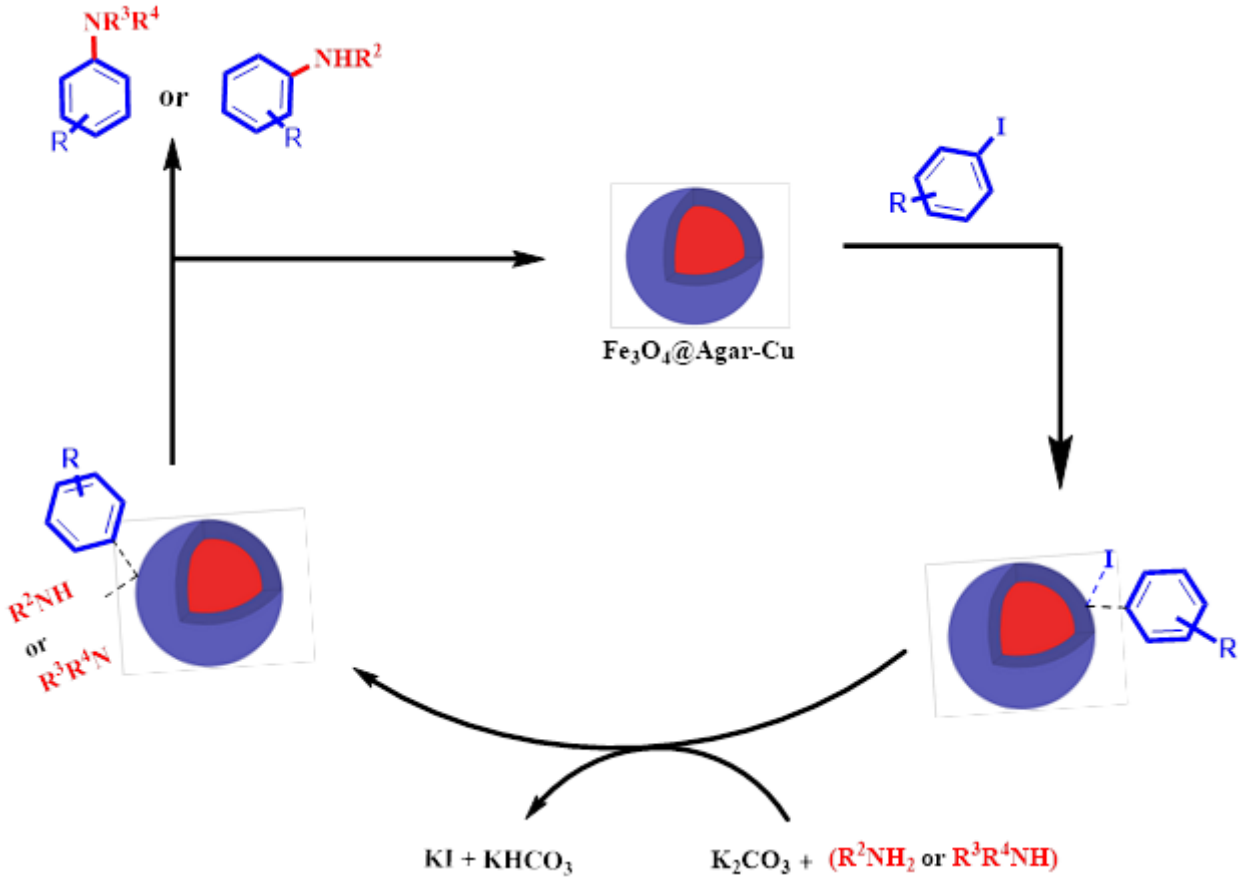


## Figure 10

The possible mechanism for cross-coupling Buchwald-Hartwig reaction in the presence of Fe3O4@Agar-Cu nanoparticles.

# Supplementary Files

This is a list of supplementary files associated with this preprint. Click to download.

- Tables.docx
- Scheme01.png
- Scheme02.png
- supportinginformation.pdf